Surface Protonation and Electrochemical Activity of Oxides in Aqueous Solution

J. B. Goodenough,* R. Manoharan, and M. Paranthaman

Contribution from the Center for Materials Science & Engineering, ETC 5.160, University of Texas at Austin, Austin, Texas 78712-1084. *Received August 15, 1989*

Abstract: Measurements of the pH dependence of the surface-charge density on oxide particles are correlated with the pH dependence of the cyclic voltammograms and of the chemical activity of the oxide for electrolysis/fuel cell reactions. Studies of the pyrochlores $Pb_2M_{2-x}Pb_xO_{7-y}$ and the rutiles MO_2 (M = Ru or Ir) and of the perovskite $Sr_{1-x}NbO_{3-\delta}$ show that (1) the oxygen-reduction reaction, found on the pyrochlores in alkaline solution, occurs by exchange of a surface OH^- species at an O′ site with an adsorbed O_2^- solution species, (2) the oxygen-evolution and chlorine-evolution reactions occur at a surface O^- species made accessible by surface oxidation of a redox couple lying close to the top of the O^{2-}:$2p^6$ valence band, and (3) the hydrogen-evolution reaction occurs at the surface OH_2 species bonded to cations with a surface redox couple lying close to the H^+/H_2 level in solution.

Several metallic oxides are known to exhibit superior electrochemical activity for at least one of the electrolysis and/or fuel-cell reactions, but the suggested reaction pathways at the oxide surface, and hence our ideas about the factors that control selectivity and reaction rates, remain speculative. For example, whether the metal atoms themselves or the surface-oxygen atoms, modified by the metal atom(s) to which they are chemically bonded, are the reaction sites remains an open question.

This paper reports, for a few selected oxides, a study of the charge on an oxide particle surface as a function of pH in aqueous solution and correlates this measurement with the electrochemical activity at the oxide surface. Our purpose is to show how these measurements can, together, provide information that not only discriminates between models of the reaction sites but also gives insight into the factors that control selectivity and reaction rates. For this initial study, we have chosen the ruthenium and iridium oxides with and without the presence of a countercation Pb^{2+} and also the defect perovskite $Sr_{1-x}NbO_{3-\delta}$. These oxides have been found to exhibit excellent performance for at least one of the electrolysis and/or fuel-cell reactions as well as for the chlorine-evolution reaction.[1-7]

Oxide Surface in Aqueous Solution

Interpretation of the data presented in this paper is based on the following model of the oxide surface. It is now well established[6,8-10] that an oxide particle binds water at the surface in order to complete the oxygen coordination of the surface metal atoms. The protons of this "bound water" become distributed over equivalent oxygen atoms on the particle surface and also come into equilibrium with the pH of any aqueous solution in which the particles are immersed. At a pH specific to the cations to which the surface oxygen are bound, the particles carry zero charge. This pH of zero charge is the point of zero-zeta potential (pzzp). At a pH < pzzp, the particles accept excess surface protons to become positively charged; at a pH > pzzp the particles donate surface protons to the solution and become negatively charged.

This description of the surface of an oxide particle in aqueous solution contains three essential features: first, there is no reconstruction of the surface of the particle; second, the surface metal atoms are only exposed to the solution through a surface oxygen; and third, the degree of protonation of the surface oxygen varies with the pH of the solution in which the particles are immersed. The first feature simplifies the problem by allowing information about the structure of the bulk oxide to be extrapolated to the surface. The second implies that the surface oxygens are the reaction sites unless a surface-oxygen species is displaced by a reactant in the solution. There is little space to "squeeze in" an extra oxygen at most fully oxygenated surfaces. The third feature suggests that a key to understanding any pH dependence of the electrochemical activity resides in a clarification of the role of the surface protons in the reaction pathways.

Two measurements provide information about the surface protonation. The first is a standard determination of the mean surface-charge density in zero applied field;[10-14] the pH at which the charge density changes sign is the pzzp of the material. The second comes from a cyclic voltammogram (CV), which provides the potential at which any quasireversible surface–redox equilibria occur for a given solution pH. The change in formal charge of the surface cation is compensated by an equivalent change in the surface-proton concentration; the latter change is responsible for carrying the current across the electrode–electrolyte interface to give the quasireversible peak in the CV. The mean surface-charge density in zero applied field corresponds to the surface protonation at the open-circuit voltage. From the model of the oxide-particle surface, it follows that the quasireversible peaks associated with surface-cation redox potentials must shift by about 60 mV/pH unit to more positive potentials in more acid solution.[5]

Finally, just as the total surface charge remains essentially constant on passing through a surface redox potential, so too it remains essentially constant through each step of a catalyzed chemical-reaction pathway. This condition provides an important constraint on the possible reaction pathways that need to be considered.

(1) Trasatti, S.; Lodi, G. *Electrodes of Conductive Metallic Oxides*; Trasatti, S., Ed.; Elsevier: New York, 1980 and 1981; Chapters 7 and 11 and references cited therein.
(2) Novak, D. M.; Tilak, B. V.; Conway, B. E. *Modern Aspects of Electrochemistry*; Bockris, J. O'M., Conway, B. E., White, R. E., Eds.; Plenum Press: New York, 1982; Chapter 4 and references cited therein.
(3) Horowitz, H. S.; Longo, J. M.; Lewandowski, J. T. U.S. Patent 4,129,525.
(4) Swette, L.; Giner, J. *J. Power Sources* **1988**, *22*, 399.
(5) Egdell, R. G.; Goodenough, J. B.; Hamnett, A.; Naish, C. C. *J. Chem. Soc., Faraday Trans. 1* **1983**, *79*, 893.
(6) Manoharan, R.; Paranthaman, M.; Goodenough, J. B. *Eur. J. Solid State Inorg. Chem.* **1989**, *26*, 155.
(7) Manoharan, R.; Goodenough, J. B. *J. Electrochem. Soc.* **1990**, *137*, 910. Manoharan, R.; Paranthaman, M.; Goodenough, J. B. 176th Meeting, The Electrochemical Society, Hollywood, Florida, 1989.
(8) England, W. A.; Cross, M. G.; Hamnett, A.; Wiseman, P. J.; Goodenough, J. B. *Solid State Ionics* **1980**, *1*, 231.
(9) Shukla, A. K.; Manoharan, R.; Goodenough, J. B. *Solid State Ionics* **1988**, *26*, 5.
(10) Furlong, D. N.; Yates, D. E.; Healey, T. W. *Electrodes of Conductive Metallic Oxides*; Trasatti, S., Ed.; Elsevier: New York, 1981; p 367.
(11) Kita, H.; Henmi, N.; Shimazu, K.; Hattori, H.; Tanabe, K. *J. Chem. Soc., Faraday Trans. 1* **1981**, *77*, 2451.
(12) Parks, G. A. *Chem. Rev.* **1965**, *65*, 177.
(13) Murray, J. W. *J. Colloid Interface Sci.* **1954**, *46*, 357.
(14) Atkinson, R. J.; Posner, A. M.; Quirk, J. P. *J. Phys. Chem.* **1967**, *71*, 550.

0002-7863/90/1512-2076$02.50/0

Experimental Section

1. Preparation of Materials and Electrodes. $Pb_2Ir_2O_{7-y}$ and $Pb_2Ru_2O_{7-y}$ were prepared by a direct solid state reaction at 850 °C from an intimate mixture of $Pb(NO_3)_2$ and Ir, and PbO and RuO_2, respectively, in stoichiometric ratio.[15] Sintered pellets (8 mm in diameter and ca. 2 mm thick) were prepared by pressing powdered materials at 900 °C for 24 h. $Sr_{1-x}NbO_{3-\delta}$ samples were prepared by heating an appropriate mixture of $SrCO_3$ and Nb_2O_5 in air to give a white product that was then intimately mixed with a stoichiometric proportion of powdered, metallic Nb. The mixture was pelletized, wrapped in tantalum foil, sealed under vacuum in a silica tube, and heated for 2 days at 1200 °C.[16] All the final products were characterized by X-ray powder diffraction with a Philips diffractometer.

The sintered pellets were polished, and copper leads were attached onto the back face with silver epoxy to an ohmic contact made of the In–Ga eutectic alloy. The sample was then mounted onto a glass holder, and ordinary epoxy resin was used to insulate from the electrolyte solution all but the front face of the pellet.

The high-surface-area $Pb_2Ir_{2-x}Pb_xO_{7-y}$ was prepared by the precipitation method of Horowitz et al.[3] A 2.2:2 molar ratio of $PbNO_3$:$IrCl_3$ was dissolved in aqueous solution at 75 °C under constant stirring. Approximately 6% KOH was added to the solution so as to maintain a pH of 13. Precipitation of the hydroxides was carried out at 75 °C under constant stirring and purging of the solution with O_2 for 24 h. The filtered product was washed several times with distilled water so as to remove any alkali present; it was then dried in an oven at 150 °C, mixed with Teflon binder, and pressed to obtain a porous electrode for electrochemical measurements.

The electrode-forming procedure was as follows:[6] Distilled water was added to a measured quantity of the catalyst precipitate. This mixture was thoroughly homogenized with a sonicator before a dilute suspension of Teflon dispersion (DuPont No. T-30 suspension) was added while the mixture was being agitated with a magnetic stirrer. The product material was centrifuged and spread on a platinum expanded-metal (exmet) screen. The coated screen was air-dried for ca. 15 min before it was cold-pressed at 125 kg/cm^2 for 5 min. The pressed mass was dried for 2 h at 110 °C and then air-cured at 360 °C for 30 min. The Teflon content of the electrodes was 25% by weight.

Deposition of a suitable quantity of $Pb_2Ru_{2-x}Pb_xO_{7-y}$ on the activated carbon was accomplished by co-precipitation from solution.[17] The purified, CO_2-activated coconut shell charcoal particles were dipped for 30 min in a 0.001 M aqueous solution of $Pb(NO_3)_2$ to obtain Pb^{2+} ions on the surface of the carbon and then for another 30 min in a solution made by first fusing for 5 min 0.1 g of RuO_2, 0.5 g of NaOH, and 5 g of KNO_3 before diluting the melt with distilled water to 250 mL. This procedure leads to a precipitation of $Pb_2Ru_{2-x}Pb_xO_{7-y}$ on the carbon surface. The particles were then washed repeatedly with distilled water and dried in an air oven at 70 °C before being mixed with the Teflon binder.

2. Electrochemical Measurements. Electrochemical measurements were made with electrodes mounted in a conventional three-electrode cell having a porous-glass separator between the working and counter electrodes. In the hydrogen evolution reaction (HER) studies, a flowing H_2 stream was passed through the electrolyte. Steady-state galvanostatic polarization data were obtained with a regulated dc power supply and a high-power decade resistance box in series with the electrochemical cell. Cyclic voltammograms were recorded with an EG&G Model 273 potentiostat interfaced to an IBM PxT microcomputer with a National Instruments IEEE-488 General-Purpose Interface (GPIB) card. The EG&G HEADSTART Creative Electrochemistry Software was used to drive the measurements, process the data, and display the cyclic voltammograms.

3. Pzzp Measurements. The point of zero-zeta potential of oxide particles prepared by solid-state reaction was determined by potentiometric base titration.[10-14] The oxide powders were suspended in 25 mL of an aqueous solution of 0.004 M KOH and 0.4 M KCl. The suspensions were titrated with 0.1 M HCl in the presence of continuous stirring and N_2 gas bubbled through the solution to prevent any contamination from the CO_2 present in the air. The end point of each point of a titration curve was determined after the pH reading became stable. Comparison of this titration curve with the one obtained with the blank solution permitted determination of the mean surface charge on the oxide particles due to protonation or deprotonation of the surface with the formula[18]

$$q^{\pm} = F\Delta VC/SW$$

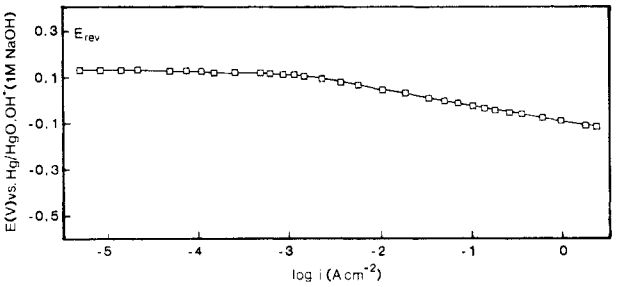

Figure 1. Tafel curve for ORR on gas-fed Teflon-bonded $Pb_2Ir_{2-x}Pb_xO_{7-y}$ in 1 M NaOH solution at 25 and 60 °C (curves were identical for the two temperatures).

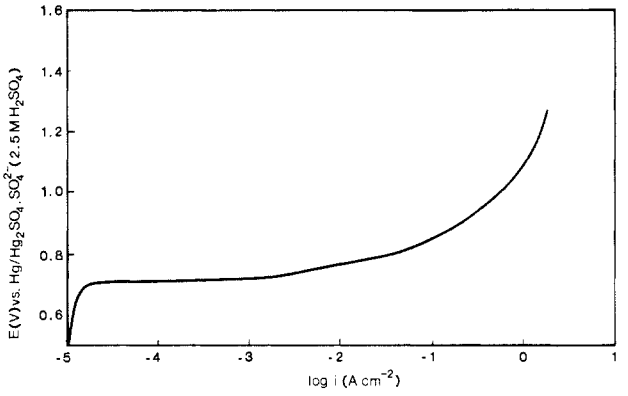

Figure 2. Tafel curve for OER on Teflon-bonded $Pb_2Ir_{2-x}Pb_xO_{7-y}$ in 2.5 M H_2SO_4 at 60 °C.

where F is Faraday's constant, ΔV is the difference in the volume of the titrant with/without the presence of powder for a given pH, C is the concentration of the titrant, S is the BET surface area, and W is the weight of the powder used.

Results and Discussion

1. The Pyrochlore $Pb_2Ir_{2-x}Pb_xO_{7-y}$. The ideal chemical formula for an oxide with the cubic pyrochlore structure is $A_2B_2O_6O'$. Like the cubic ABO_3 perovskite, it contains a B_2O_6 framework of corner-shared BO_6 octahedra, but a cooperative buckling of the framework changes the B–O–B bond angle from 180° to about 135°. The buckling opens up the interstitial space to allow occupancy by O′ oxygen atoms as well as the larger A cations. The interstitial A_2O' array consists of corner-shared $O'A_4$ tetrahedra. The essential feature is the B_2O_6 framework; the interstitial space may be variously occupied. For example, antimonic acid $Sb_2O_5{\cdot}4H_2O$ has an Sb_2O_6 pyrochlore framework with A = H_3O^+ and O′ = H_2O.[8]

The pyrochlore $Pb_2Ir_2O_{7-y}$ contains Pb^{2+} ions on the A sites; a $y \approx 0.9$ leaves the O′ sites almost completely vacant in the bulk.[15] As normally prepared, some Pb is incorporated into the framework as Pb^{4+} to give the general chemical formula $Pb_2Ir_{2-x}Pb_xO_6O'_{1-y}$. This metallic oxide is a good catalyst for the oxygen-reduction reaction (ORR) in alkaline solution and for the oxygen-evolution reaction (OER) in acid solution.[3,4,6] Polarization curves for these two reactions are shown in Figures 1 and 2, respectively. Data points were obtained by raising the current to each successive point and waiting for 5 min. The current was shut off after the terminal point, and the original curve was reproduced once the open-circuit voltage at zero current had stabilized at its original value. A Tafel slope of 60 mV/decade ($2.3RT/F$) was found for each reaction at higher current densities. The initial region of the Tafel curve in Figure 1 presumably represents a charging of the pseudocapacitance and may also be associated with the formation of O_2^-. In Figure 2, the Tafel slope of 60 mV/decade extends over only 1.5 decades, but this result is without the mass-transfer correction. In Figure 1, we also observe temperature-independent behavior

(15) Longo, J. M.; Raccah, P. M.; Goodenough, J. B. *Mater. Res. Bull.* **1969**, *4*, 191.
(16) Ridgley, D.; Ward, R. J. *J. Am. Chem. Soc.* **1955**, *77*, 6132.
(17) Goodenough, J. B.; Shukla, A. K.; Palitiero, C.; Jamieson, K. R.; Hamnett, A.; Manoharan, R. British Patent 8422546.
(18) Bockris, J. O'M.; Otagawa, T. *J. Electrochem. Soc.* **1986**, *131*, 290.

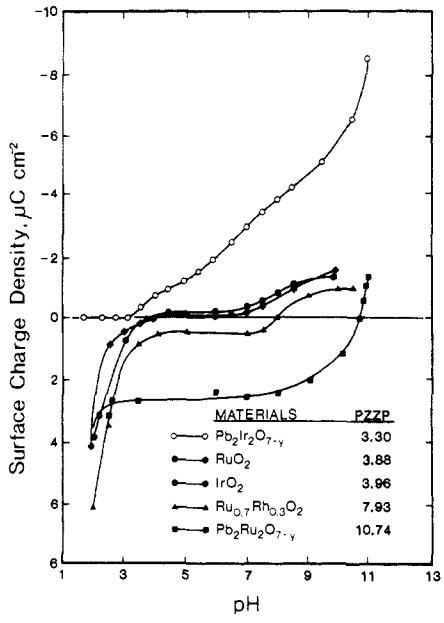

Figure 3. Surface-charge densities of various iridium and ruthenium oxides immersed in aqueous solutions. All the data have been collected with a solution of constant ionic strength.

between 25 and 60 °C. As pointed out by Horowitz et al.,[19] this probably results from the fortuitous compensation of an Arrhenius behavior by a decrease in either the hydrophobicity of the electrode or the oxygen solubility of the electrolyte with increasing temperature.

On the other hand, this oxide does not reduce O_2 in acid solution, and corrosion accompanies an inefficient O_2 evolution in alkaline solution.[4] These data invite an investigation into the role of the solution pH.

The pH dependence of the mean surface-charge density of $Pb_2Ir_2O_{7-y}$ is shown in Figure 3. A most unusual feature of these data is the absence of any observable positive charge on the particles for a pH < pzzp = 3.30. This observation indicates that the pyrochlore $Pb_2Ir_2O_6O'_{1-y}$ binds water at a set of surface sites that are essentially vacant in the as-prepared sample and that the other surface oxygens are too acidic to accept protons in zero applied voltage in the experimental range of pH ≥ 1.5. Since a $y \approx 0.9$ gives only about 10% occupancy of the O′ sites in the bulk, it follows immediately that it is the surface O′ oxygens that are missing in the dry particles. The strongly bound O oxygens of the Ir_2O_6 framework are acidic because of the inductive effect. We may therefore conclude that in solution the surface O′ sites become occupied by "bound-water" molecules that retain their protons in a pH < pzzp ≈ 3.30; protons are donated from this water to a solution of pH > 3.30, which charges the particles negatively. The O oxygens of the Ir_2O_6 framework remain unprotonated in zero applied field for pH ≥ 1.5, but we should anticipate a protonation of these oxygens setting in at pH < 1.5 by extrapolation of the surface-charge density vs pH of IrO_2 in Figure 3.

The CV obtained in 2.5 M H_2SO_4 is shown in Figure 4a. A slow cathodic drift of the open-circuit voltage to a −0.225 V versus the standard calomel electrode (SCE) indicates that in 2.5 M H_2SO_4 the O oxygens of the Ir_2O_6 are indeed protonated in zero applied field. The CV exhibits two quasireversible peaks corresponding to the surface Ir (4+/3+) couple between +0.1 and +0.3 V (average ca. +0.2 V) and the Ir(5+/4+) couple between 0.75 and +0.93 V (average ca. +0.84 V) relative to the SCE. An irreversible OER starts at about +1.12 V; there is no evidence of an ORR in the CV. On changing the cathodic limit of the cyclic range from −0.225 to −0.625 V vs SCE, there is a topotactic extrusion of Pb from the oxide;[6] the vacant O′ sites allow room

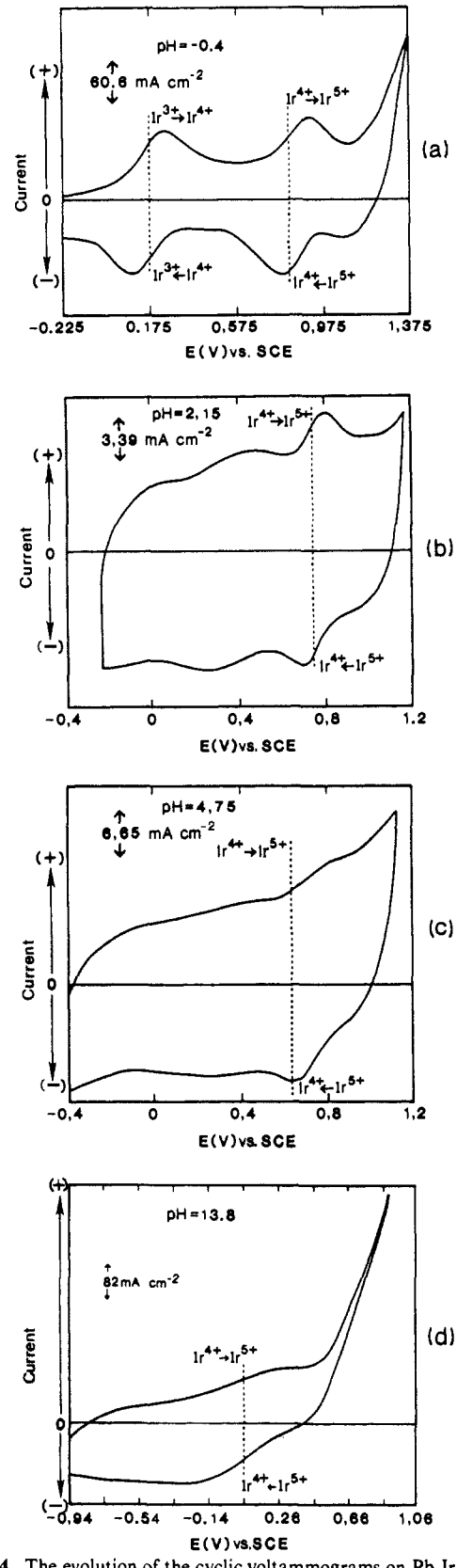

Figure 4. The evolution of the cyclic voltammograms on $Pb_2Ir_2O_{7-y}$ with changing pH: (a, b, and d) at 100 mV s^{-1} and (c) at 50 mV s^{-1}.

temperature mobility of Pb^{2+} ions in the interstitial space of the Ir_2O_6 framework.[20]

It is instructive to monitor the evolution of the CV with changing pH (Figure 4). At pH > 1.5, the Ir_2O_6 framework is not pro-

(19) Horowitz, H. S.; Longo, J. M.; Horowitz, H. H. *J. Electrochem. Soc.* **1983**, *130*, 1851.

(20) Goodenough, J. B.; Hong, H. Y. P.; Kaflas, J. A. *Mater. Res. Bull.* **1976**, *11*, 203.

tonated at open-circuit voltage according to our interpretation of Figure 3, and the peak assigned to the surface Ir(4+/3+) couple in Figure 4a has disappeared in Figure 4b–d. However, the peak assigned to the surface Ir(5+/4+) couple remains and is shifted cathodically by about 60 mV/pH unit as expected. At pH > 1.5, the surface proton donated to the solution to compensate for the $Ir^{4+} \rightarrow Ir^{5+}$ valence change at the surface would have to come from the water at an O′ site. In 1 M NaOH, Figure 4d, the CV exhibits only this one quasireversible peak at an estimated average position of +0.04 V (SCE); it is broadened and partially obscured by a diffuse, irreversible cathodic peak that can be assigned to the ORR.[6] An irreversible OER occurring in the region anodic of +0.46 V (SCE) is similarly shifted to more negative potential by about 60 mV/pH unit relative to its position in 2.5 M H_2SO_4. The broad, irreversible peak associated with the ORR is still present in pH = 4.75 > pzzp, but by pH = 2.15 < pzzp it has disappeared. The quasireversible peak near +0.35 V (SCE) for pH = 2.15 would seem to represent a reversible electron transfer to the dioxygen molecule, the first step in the ORR, see (1) below.

From these data and the model of the oxide surface, we draw the following conclusions:[6] First, the ORR occurs via a displacement of OH^- ions at O′ sites in a solution of pH > pzzp; complete protonation to H_2O of the oxygen at these sites in a solution of pH < pzzp blocks the rate-determining step (rds) in the reaction sequence.

$$O_2 + e^- \rightarrow O_2^-{}_{ads}$$

$$Pb^{2+}OH^- + O_2^-{}_{ads} \xrightarrow{rds} Pb^{2+}O_2^- + OH^- \qquad (1)$$

$$Pb^{2+}O_2^- + 2H_2O + 3e^- \rightarrow Pb^{2+}OH^- + 3OH^-$$

The O oxygens of the Ir_2O_6 framework are too tightly bound to the iridium ions to participate in the displacement reaction of the ORR. Second, the OER occurs, on the other hand, at a deprotonated surface oxygen anodic of the surface Ir(5+/4+) redox couple. In 2.5 M H_2SO_4, the reaction sequence could be

$$Ir^{4+}OH^- \rightarrow Ir^{5+}O^{2-} + H^+_{aq} + e^-$$

$$Ir^{5+}O^{2-} \rightleftharpoons Ir^{4+}O^- \qquad (2)$$

$$Ir^{4+}O^- + H_2O \rightarrow Ir^{4+}OOH^- + H^+_{aq} + e^-$$

$$2Ir^{4+}OOH^- \xrightarrow{rds} 2Ir^{4+}OH^- + O_2\uparrow$$

but for 1.5 < pH < 3.3, and perhaps at 2.5 M H_2SO_4 also, the sequence would be more complex

$$Ir^{4+}O^{2-} + Pb^{2+}OH_2 \rightarrow Ir^{5+}O^{2-} + Pb^{2+}OH^- + H^+_{aq} + e^-$$

$$Ir^{5+}O^{2-} \rightleftharpoons Ir^{4+}O^- \qquad (2')$$

$$Ir^{4+}O^- + H_2O \rightarrow Ir^{4+}OO^{2-} + Pb^{2+}OH_2 + H^+_{aq} + e^-$$

$$2Ir^{4+}OO^{2-} \xrightarrow{rds} 2Ir^{4+}O^{2-} + O_2\uparrow$$

as it involves the transfer of a proton from the O′ oxygen. For pH > 3.3, a $Pb^{2+}OH^-$ species could be involved in reaction 2′.

In order to test further the first of these conclusions, we investigated the ORR at pH = 2.15 and 4.75. As predicted, there is no activity at pH = 2.15 < pzzp where the O′ sites are fully protonated to H_2O according to our analysis of Figure 3, but there is a weak activity at pH = 4.75 > pzzp where some protons are donated from the O′ oxygen to the solution.

2. The Pyrochlore $Pb_2Ru_{2-x}Pb_xO_{7-y}$. The ruthenium oxide pyrochlore is similar to the iridium oxide analogue. However, a $y \approx 0.5$, which manifests itself as an ordering of vacancies in the O′ sites in $Pb_2Ru_2O_{6.5}$,[15] leaves the surface O′ sites partially occupied by oxygen in the dry state. This change in O′-site occupancy has a dramatic effect on the plot of surface-charge density versus pH (Figure 3), since full protonation to H_2O of all the oxygens at O′ sites must, in this case, charge the particles positively. A shift of the pzzp to 10.74 and a sharp crossing from negative to positive surface-charge density are thus seen to be consistent, within our model, with a half-occupancy of the O′ sites in bulk $Pb_2Ru_2O_{6.5}$. Extrapolation from the curve for the surface-charge density of RuO_2 versus pH in Figure 3 indicates that we must anticipate the onset of protonation of the O oxygen of the Ru_2O_6 framework in more acid solution, and there is an indication that this protonation is setting in for pH ≤ 2.

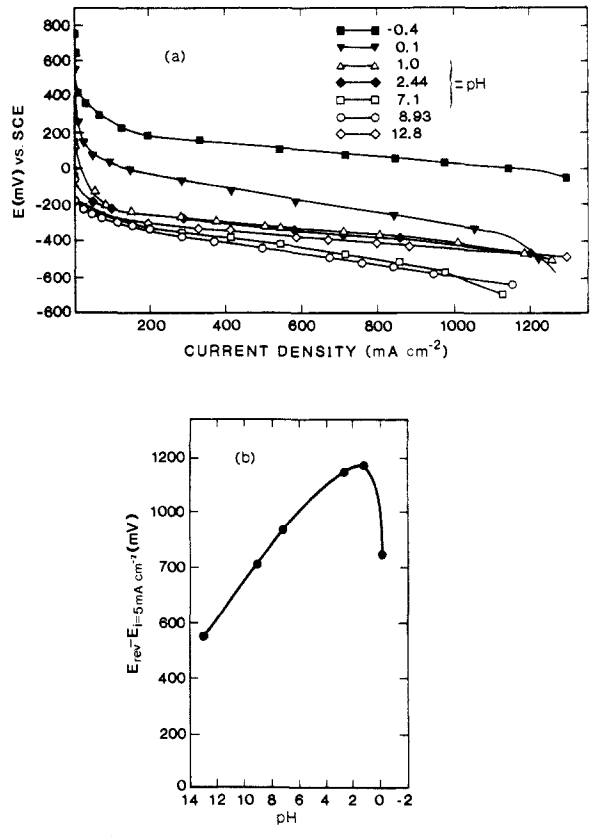

Figure 5. (a) Oxygen-reduction polarization curves for $Pb_2Ru_{2-x}Pb_xO_{7-y}$ on treated carbon at 60 °C as a function of pH and (b) variation with electrolyte pH of the ORR activity at low current density. The ionic strength of the electrolyte was maintained constant by adding either H_2SO_4 or NaOH solution to 0.5 M Na_2SO_4 solution.

This pyrochlore is also active for the ORR in alkaline solution; in fact, very high current densities have been sustained for this reaction in 1 M KOH with gas-activated coconut-shell charcoal impregnated with a $Pb_2Ru_{2-x}Pb_xO_{7-y}$ catalyst.[17] Unfortunately the pyrochlore ruthenium oxide electrodes are slightly soluble in strong alkali solutions. More fundamental for this study is the variation of the ORR with pH. The polarization measurements of Figure 5 were made with a single electrode, which keeps all variables fixed except the solution pH. They show that the ORR is reduced, but not totally suppressed, in acid solution; but they also indicate a change in the dominant ORR mechanism in a narrow pH range about pH 2. From the variation with pH in the surface-charge density, we can now interpret the change in mechanism to be a change in the reaction site where the rate-determining exchange reaction occurs. At pH > 2, the Ru_2O_6 framework is unprotonated and the exchange reaction can only occur at $Pb^{2+}OH^-$ sites, which decrease in concentration with decreasing pH as they become more converted to $Pb^{2+}OH_2$ sites. At pH < 2, protonation of the Ru_2O_6 framework sets in and increases with decreasing pH. It would thus appear that either the OH^- groups on an Ru_2O_6 framework, unlike those on an Ir_2O_6 framework, are not too tightly bound to participate in the exchange reaction

$$Ru^{3+}OH^- + O_2^-{}_{ads} \xrightarrow{rds} Ru^{3+}O_2^- + OH^- \qquad (1')$$

or, as appears more likely (see below), in pH < 2 a surface restructuring occurs that allows such a reaction to sustain the ORR into acid solution at some new type of surface oxygen, e.g. a terminal as against a bridging oxygen.

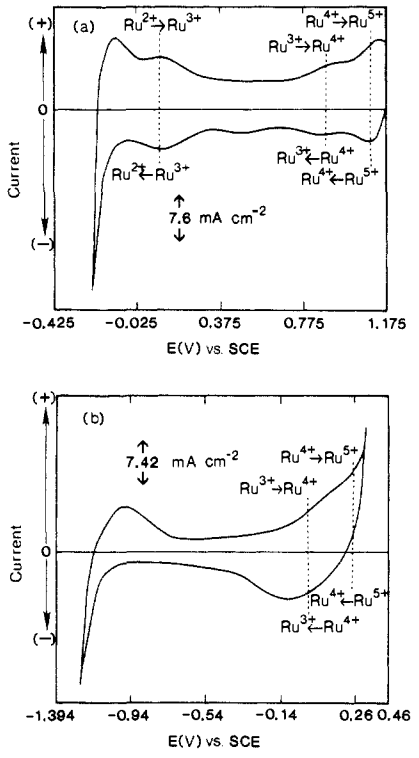

Figure 6. Cyclic voltammograms for $Pb_2Ru_2O_{7-y}$ in (a) 2.5 M H_2SO_4 and (b) 1 M NaOH, both at 25 °C; scan rate 25 mV s^{-1}.

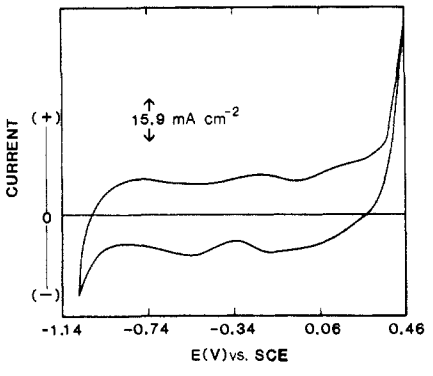

Figure 7. Cyclic voltammograms for $Pb_2Ru_2O_{7-y}$ (first cycle) obtained in 1 M NaOH at 25 °C after cycling in acid solution.

The CVs in 2.5 M H_2SO_4 and 1 M KOH are shown in Figure 6. In acid, three quasireversible peaks can be seen; as reported for RuO_2,[21-26] they correspond to a surface Ru(3+/2+) redox couple at about +0.1 V, a Ru(4+/3+) couple at about +0.9 V, and a Ru(5+/4+) couple at about +1.1 V (SCE). The Ru(5+/4+) couple just precedes the OER in the anodic sweep. In alkaline solution, where the Ru_2O_6 framework is unprotonated, the Ru(4+/3+) and Ru(5+/4+) couples are shifted to more negative potential with the OER by about 60 mV/pH unit and the Ru(3+/2+) couple appears to be suppressed. However, on placing an electrode into alkaline solution after being in acid, the first CV cycle was obtained as shown in Figure 7. The CV of Figure 6b is recovered after several cycles. Moreover, enhanced capacitive currents are found in acid, which is suggestive of an increase in surface roughness. These observations suggest that, in pH < 2, some other alteration of the surface is occurring than that envisaged by our ideal model. Nevertheless, the existence of an OER just anodic of the Ru(5+/4+) surface couple implies that the reaction pathway is similar to that given in (2) or (2′) above for the iridium analogue.

3. Rutile RuO_2 and IrO_2. Both RuO_2 and IrO_2 have the rutile structure and are reported to exhibit very good performance as electrodes in a number of electrochemical applications.[1,2,25-30] They both tend to undergo corrosion under anodic potentials in alkaline solution whereas they are quite stable in acid.

In the range 4 < pH < 7, the surface-charge density on these particles is nearly zero (Figure 3), which suggests that these oxides also have a set of distinguishable sites that are nearly all vacant in the dry state. It is more difficult to identify these sites with certainty since the bulk oxygens are all energetically equivalent. However, two types of surface oxygen are present: bridging and terminal oxygen. The bridging oxygen would be more tightly bound and hence more acidic; we therefore assume that, on these oxides, the terminal oxygens are mostly missing in the dry state. In solution, these sites are occupied by the oxygen of water molecules; and in acid, they are protonated to H_2O to leave the particles nearly neutral in the range 4 < pH < 7. Protonation of the bridging oxygen sets in for pH < 4, in particular for pH < pzzp. If the bridging oxygens are too tightly bound to participate in an exchange reaction like (1′), we cannot expect to find an ORR in acid solution where the terminal oxygens are fully protonated to water, and none is found.

However, in alkaline solution an ORR on RuO_2 has been reported.[3,31-33] According to Yeager et al.,[31,33] the ORR involves primarily the formation of hydrogen peroxide, but dissolution of the electrode kept them from obtaining precise information. Horowitz et al.[3] showed that a superior ORR activity occurs on amorphous $RuO_2{\cdot}H_2O$, but the best ORR remained inferior to that obtained on $Pb_2Ru_{2-x}Pb_xO_{7-y}$. From our interpretation of the data of Figure 3, the terminal oxygen O_t at the surface of an RuO_2 particle corresponds to the oxygen on O′ sites in the pyrochlore. We must expect a higher density of O_t oxygen on amorphous $RuO_2{\cdot}H_2O$ than on RuO_2 itself. Moreover, these sites are not fully protonated to H_2O for pH > 7. Therefore, in alkaline solution we may have the ORR occurring at $Ru^{3+}O_tH^-$ species in RuO_2 and $RuO_2{\cdot}H_2O$ in analogy with the ORR occurring at $Pb^{2+}OH^-$ sites in the pyrochlores. If the final steps in reaction 1 were written out in detail, we would have

$$Ru^{3+}O_tH^- + O_2^- \xrightarrow{rds} Ru^{3+}O_2^- + OH^-$$

$$Ru^{3+}O_2^- + H_2O + e^- \rightarrow Ru^{3+}OOH^- + OH^-$$

$$Ru^{3+}OOH^- + H_2O \rightarrow Ru^{3+}OH^- + H_2O_2 \qquad (1'')$$

with the final chemical step competing with the electrochemical reaction

$$Ru^{3+}OOH^- + H_2O + 2e^- \rightarrow Ru^{3+}OH^- + 2OH^-$$

In acid solution, RuO_2 evolves O_2 well and the activity for Cl_2 evolution is excellent. RuO_2 also evolves H_2 very well in acid,[34-36]

(21) Trasatti, S.; Buzzanca, G. *J. Electroanal. Chem.* **1971**, *29*, App.1.
(22) Arikado, T.; Iwakure, C.; Tamura, H. *Electrochim. Acta* **1977**, *22*, 217.
(23) Burke, L. D.; Murphy, O. J.; O'Neil, J. F.; Venkatesan, S. *J. Chem. Soc., Faraday Trans. 1* **1977**, *73*, 1659.
(24) Kokonlina, D. V.; Ivanova, T. V.; Krasovitskaya, Yu. I.; Kudryavtseva, Z. I.; Krishtalik, L. I. *Elektrokhimiya* **1977**, *13*, 1511.
(25) Doblhofer, K.; Metikos, M.; Ogami, Z.; Gerischer, H. *Ber. Busenges. Phys. Chem.* **1978**, *82*, 1046.
(26) Burke, L. D.; Murphy, O. J. *J. Electroanal. Chem.* **1979**, *96*, 19.
(27) Loutfy, R. O.; Leroy, R. L. *J. Appl. Electrochem.* **1978**, *8*, 549.
(28) Khodkevich, S. D.; Zhukova, L. N.; Yakimenko, L. M.; Kubasov, V. L.; Ivanter, I. A. *Elektrokhimiya* **1977**, *13*, 38.
(29) Elina, M.; Gitneva, V. M.; Bystrov, V. I. *Elektrokhimiya* **1975**, *11*, 1279.
(30) Fioshin, M. Ya.; Avrutskaya, I. A.; Malachova, T. A.; Mulina, T. E. *Elektrokhimiya* **1974**, *10*, 796.
(31) O'Grady, W. E.; Iwakura, C.; Huang, J.; Yeager, E. *Electrocatalysis*; The Electrochemical Society: Princeton, NJ, *1974*; p 286.
(32) Horkans, J.; Shafer, M. W. *J. Electrochem. Soc.* **1977**, *124*, 1202.
(33) Yeager, E. *Natl. Bur. Stand. Spec. Publ.* **1976**, *455*, 203.
(34) Galizzioli, D.; Tantardimi, F.; Trasatti, S. *J. Appl. Electrochem.* **1975**, *5*, 203.
(35) Kotz, E. R.; Stucki, S. *J. Appl. Electrochem.* **1987**, *17*, 1190.
(36) Manoharan, R.; Paranthaman, M.; Goodenough, J. B. Unpublished results.

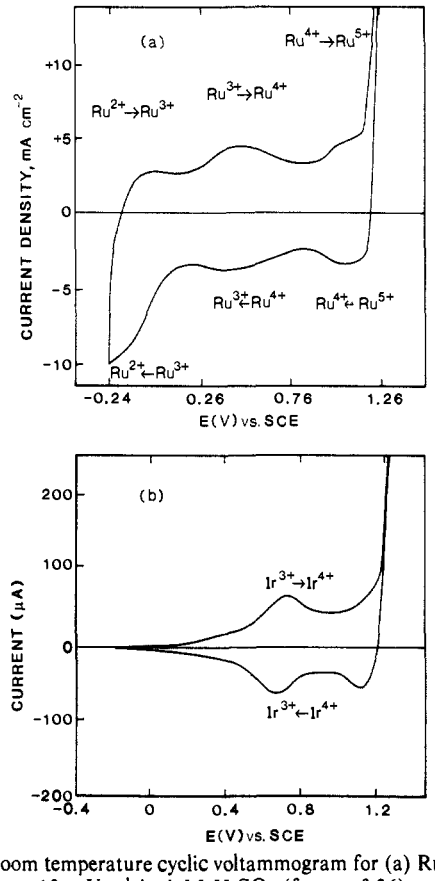

Figure 8. Room temperature cyclic voltammogram for (a) RuO_2-coated Ti substrate at 19 mV s^{-1} in 1 M H_2SO_4 (from ref 26) and (b) IrO_2 electrode at 100 mV s^{-1} in 0.5 M H_2SO_4 (from ref 34).

and it is possible to obtain the reversible potential of hydrogen after a strong hydrogen discharge in H_2-saturated solution. The activities of IrO_2 for these reactions are only slightly inferior to those of RuO_2.[1,2,36,37]

Figure 8 compares the CVs of RuO_2 and IrO_2 in acid. Within the potential range between hydrogen and oxygen (or chlorine) evolution, RuO_2 exhibits three quasireversible peaks corresponding to the surface Ru(3+/2+), Ru(4+/3+), and Ru(5+/4+) couples.[21-26] In this oxide also the Ru(5+/4+) couple precedes the OER in the anodic sweep, and we conclude that the OER on RuO_2 proceeds by a reaction pathway similar to that on the pyrochlores where it is important that the equilibrium

$$Ru^{5+}O^{2-} \rightleftharpoons Ru^{4+}O^{-} \qquad (3)$$

is not biased too strongly to the left. In the case of IrO_2, on the other hand, the surface appears to be equilibrated only between Ir^{3+} and Ir^{4+},[38-41] but the position of the quasireversible peak is close to the voltage of the surface Ir(5+/4+) couple on the pyrochlore. Therefore we suspect that the pathway of the OER on IrO_2 is similar to that on the pyrochlore where the critical equilibrium is

$$Ir^{5+}O^{2-} \rightleftharpoons Ir^{4+}O^{-} \qquad (4)$$

The situation is similar for Cl_2 evolution on RuO_2 or IrO_2. The reversible potential for Cl_2 evolution is 0.13 V anodic of that for O_2 evolution, so equilibriums 3 and 4 are established on the surfaces of RuO_2 and IrO_2 at the potential of Cl_2 evolution. In the case of RuO_2, the steps of Cl_2 evolution that follow would be

$$Ru^{4+}O^{-} + Cl^{-} \rightarrow Ru^{4+}OCl^{-} + e^{-}$$
$$Ru^{4+}OCl^{-} + Cl^{-} \rightarrow Ru^{5+}O^{2-} + Cl_2\uparrow + e^{-} \qquad (5)$$

or

$$2Ru^{4+}OCl^{-} \rightarrow 2Ru^{5+}O^{2-} + Cl_2\uparrow$$

with an analogous reaction sequence for IrO_2. This mechanism differs from those that have been proposed in the literature.[1,2,42-45]

We turn finally to the hydrogen-evolution reaction. In acid, both the RuO_2 and the IrO_2 surfaces are protonated according to Figure 3, and we may envisage for RuO_2 the reaction

$$Ru^{3+}OH^{-} + H^{+}_{aq} + e^{-} \rightarrow Ru^{2+}OH_2$$
$$2Ru^{2+}OH_2 \rightarrow 2Ru^{3+}OH^{-} + H_2 \qquad (6)$$

and/or

$$Ru^{2+}OH_2 + H^{+}_{aq} + e^{-} \rightarrow Ru^{3+}OH^{-} + H_2$$

since the surface Ru(3+/2+) couple precedes the HER on the cathodic sweep.

Substitution of Ru by Rh in $Ru_{2-x}Rh_xO_2$ increases the pzzp in a manner that suggests the presence of O_t on rhodium in the dry state. Protonation of the bridging oxygen occurs at about the same pH as for RuO_2 and IrO_2, and the HER on this material is similar.

4. The Defect Perovskite $Sr_{1-x}NbO_{3-\delta}$. Metallic $Sr_{1-x}NbO_{3-\delta}$ ($0.05 \le x \le 0.3$) has a maximum strontium concentration at $x = 0.05$.[16] This defect perovskite is stable in acid, and $Sr_{0.95}NbO_{3-\delta}$ is a good catalyst for the HER in 2.5 M H_2SO_4, as can be seen from the CV in Figure 9. No reaction other than the HER occurs on this oxide.[7] Samples with $x > 0.05$ gave similar results, but were less active.

It is well-known that the 4d band of this oxide lies several electron volts above the top of the O^{2-}:$2p^6$ valence band, so the equilibrium

$$Nb^{5+}O^{2-} \rightleftharpoons Nb^{4+}O^{-}$$

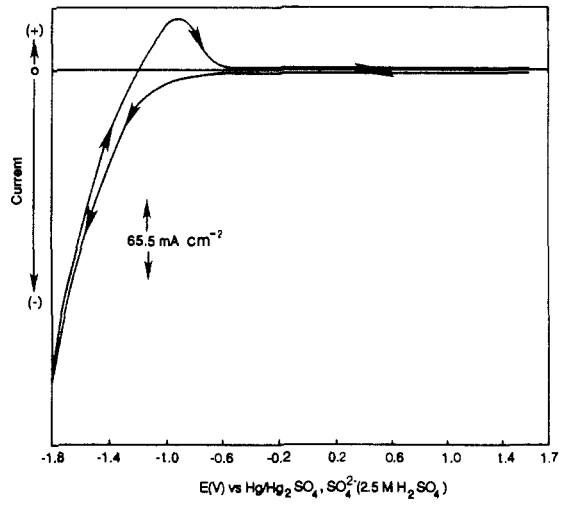

Figure 9. Room temperature cyclic voltammogram for $Sr_{0.95}NbO_{3-\delta}$ at 100 mV s^{-1} in 2.5 M H_2SO_4.

(37) Boodts, J. C. F.; Trasatti, S. *J. Appl. Electrochem.* **1989**, *19*, 255.
(38) Hackwood, S.; Schiavone, L. M.; Dautremont-Smith, W. C.; Beni, G. *Proceedings of the Symposium on Electrocatalysis*; O'Grady, W. E., Ross, P. N., Will, F. G., Eds.; The Electrochemical Society: Princeton, NJ, 1982; p 198.
(39) Gottesfeld, S.; Srinivasan, S. *J. Electroanal. Chem.* **1978**, *86*, 89.
(40) Buckley, D. N.; Burke, L. D. *J. Chem. Soc., Faraday Trans. 1* **1975**, *71*, 1447.
(41) Burke, L. D. *Electrodes of Conductive Metallic Oxides*; Trasatti, S., Ed.; Elsevier: New York, 1980; p 141 and references cited therein.
(42) Arikado, T.; Iwakura, C.; Tamura, H. *Electrochim. Acta* **1977**, *22*, 229.
(43) Arikado, T.; Iwakura, C.; Tamura, H. *Electrochim. Acta* **1978**, *23*, 9.
(44) Augustynski, J.; Balsenc, L.; Hinden, J. *J. Electrochem. Soc.* **1978**, *125*, 1093.
(45) Janssen, L. J.; Starmans, L. M. C.; Vissher, J. G.; Barendrecht, E. *Electrochim. Acta* **1977**, *22*, 1093.

is biased strongly to the left. Therefore we could not expect to find an OER according to our model. Moreover, the oxygens of the NbO_3 framework are too tightly bound to participate in an exchange reaction with an $O_2^-{}_{ads}$ species, so we also cannot expect an ORR. On the other hand, the surface-charge density (Figure 10) becomes sharply positive below a critical pH, which shows that the surface is strongly protonated in acid. Therefore we should expect a HER to occur, especially as the Fermi energy in this oxide is close to the H^+/H_2 energy level in solution. We have found that the activity for the HER decreases with increasing x, i.e., with increasing Nb^{5+}/Nb^{4+} ratio. From Figure 10, the onset of protonation in zero applied field moves to lower pH with increasing x, as would be expected for a higher mean formal charge on the niobium ions. The activity of the HER is thus clearly correlated with the degree of protonation of the surface oxygen.

Since niobium can form a short Nb–O bond within an octahedral site, we assume that the terminal oxygens form the short bond and are therefore acidic. (Such an assumption is not critical, but with it we focus on the bridging oxygen.) We may then write in analogy with eq 3 the reaction

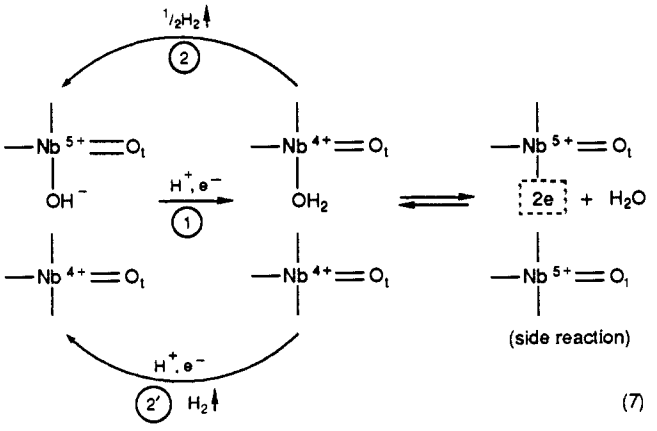

(7)

where we cannot choose unambiguously whether the second step is via pathway 2 or 2′. The point we wish to stress here is that the reaction appears to take place on a surface oxygen as the reaction site. The side reaction, shown in eq 7, is postulated to take account of the anomalous peak in the anodic sweep of the CV (Figure 9).

Conclusions

We draw the following conclusions from this work:

(1) Measurement of the surface-charge density of an oxide particle versus pH provides useful supplemental information about chemical-reacton pathways catalyzed on the oxide surface.

(2) The ORR proceeds via an exchange between a surface OH^- species and an adsorbed $O_2^-{}_{ads}$ solution species. For this exchange reaction to proceed at any appreciable rate, the surface OH^- species must be present in high concentration and not too tightly bound to the surface. Where the surface OH^- species are bridging units in a strongly bonded framework, they are not active. In the pyrochlore structure, the OH^- species at O′ sites are active; but on lead pyrochlores in acid, protonation of these sites to OH_2 blocks their activity. On RuO_2, the terminal O_t oxygens are analogous to the oxygens at O′ sites in the pyrochlores.

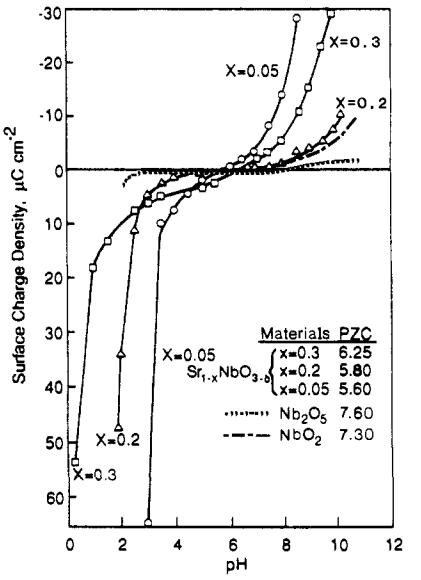

Figure 10. Surface-charge densities of $Sr_{1-x}NbO_{3-\delta}$, Nb_2O_5, and NbO_2 in aqueous solutions. All the data have been collected for powders immersed in aqueous solution of constant ionic strength.

(3) The reactive site in the OER on an oxide is a surface O^- species. Stabilization of this species requires oxidation of a surface cation to a redox couple lying close to the top of the O^{2-}:$2p^6$ valence band; in this situation, the equilibrium

$$M^{(m+1)+}O^{2-} \rightleftharpoons M^{m+}O^-$$

is not shifted too far to the left. On ruthenium and iridium oxides, the surface redox couples Ru(5+/4+) and Ir(5+/4+) satisfy this criterion; but the Nb(5+/4+) couple in $Sr_{0.95}NbO_{3-\delta}$ does not.

(4) The reactive site for the chlorine-evolution reaction is the same as that for the OER, a surface O^- species.

(5) The surface oxygen atoms are also the reactive sites in the HER on an oxide. However, strong protonation of the oxide surface is required, which favors an acid solution, as well as a cation redox couple near the H^+/H_2 level in solution.

Acknowledgment. We thank the Robert A. Welch Foundation, Houston, TX, for partial support of this work and A. Hamnett for his discussions in the early stages of our work on the $Pb_2Ru_{2-x}Pb_xO_{7-y}$ pyrochlores.